One-Step Method for Generating PEG-Like Plasma Polymer Gradients: Chemical Characterization and Analysis of Protein Interactions

ARTICLE *in* LANGMUIR · SEPTEMBER 2010

Impact Factor: 4.46 · DOI: 10.1021/la102033d · Source: PubMed

11 AUTHORS, INCLUDING:

Donna Menzies
The Commonwealth Scientific and Industrial…
13 PUBLICATIONS **170** CITATIONS
SEE PROFILE

Bruce Cowie
Australian Synchrotron
102 PUBLICATIONS **1,916** CITATIONS
SEE PROFILE

Ljiljana Puskar
Australian Synchrotron
42 PUBLICATIONS **414** CITATIONS
SEE PROFILE

Marcus Textor
ETH Zurich
334 PUBLICATIONS **14,060** CITATIONS
SEE PROFILE

Langmuir
Article
pubs.acs.org/Langmuir

One-Step Method for Generating PEG-Like Plasma Polymer Gradients: Chemical Characterization and Analysis of Protein Interactions

Donna J. Menzies,[†,‡] Bruce Cowie,[∥] Celesta Fong,[†] John S. Forsythe,[‡] Thomas R. Gengenbach,[†] Keith M. McLean,[†] Ljiljana Puskar,[∥] Marcus Textor,[§] Lars Thomsen,[∥] Mark Tobin,[∥] and Benjamin W. Muir*[,†]

[†]*CSIRO, Molecular and Health Technologies, Clayton, Victoria 3168, Australia,* [‡]*Department of Materials Engineering, Monash University, Clayton, Victoria 3800, Australia,* [§]*Laboratory for Surface Science and Technology, Department of Materials, ETH, 8093 Zurich, Switzerland, and* [∥]*Australian Synchrotron, Clayton, Victoria 3168, Australia*

Received May 19, 2010. Revised Manuscript Received July 9, 2010

In this work we report a one-step method for the fabrication of poly(ethylene glycol) PEG-like chemical gradients, which were deposited via continuous wave radio frequency glow discharge plasma polymerization of diethylene glycol dimethyl ether (DG). A knife edge top electrode was used to produce the gradient coatings at plasma load powers of 5 and 30 W. The chemistry across the gradients was analyzed using a number of complementary techniques including spatially resolved synchrotron source grazing incidence FTIR microspectroscopy, X-ray photoelectron spectroscopy (XPS) and synchrotron source near edge X-ray absorption fine structure (NEXAFS) spectroscopy. Gradients deposited at lower load power retained a higher degree of monomer like functionality as did the central region directly underneath the knife edge electrode of each gradient film. Surface derivatization experiments were employed to investigate the concentration of residual ether units in the films. In addition, surface derivatization was used to investigate the reactivity of the gradient films toward primary amine groups in a graft copolymer of poly (L-lysine) and poly(ethylene glycol) (PLL-*g*-PEG copolymer) which was correlated to residual aldehyde, ketone and carboxylic acid functionalities within the films. The protein adsorption characteristics of the gradients were analyzed using three proteins of varying size and charge. Protein adsorption varied and was dependent on the chemistry and the physical properties (such as size and charge) of the proteins. A correlation between the concentration of ether functionality and the protein fouling characteristics along the gradient films was observed. The gradient coating technique developed in this work allows for the efficient and high-throughput study of biomaterial gradient coating interactions.

Introduction

The use of surface chemistry gradients to interrogate and optimize material-biological interactions in a high-throughput manner has become an increasingly popular tool in the field of biomaterials research. The generation of surface chemistry gradients can provide information on multiple compositions in a single experiment. Factors such as chemical functionality,[1−3] wettability,[4−6] topography,[5,7] surface charge,[8] molecular structure,[9,10] and the resulting physical properties[11,12] that may influence the interaction of biomolecules and cells can be tested while minimizing experimental error. Furthermore, there are a number of physiological and biological processes which are driven by chemical gradient stimuli, such as the maintenance of homeostatic equilibrium, chemotaxis,[13] and embryonic development via gradient induced cell proliferation and differentiation. Tissue formation and neuronal development[14,15] are also controlled by a gradient distribution of specific biological cues[15,16] in vivo. Therefore surfaces that are able to mimic this physiological organization in vitro are of considerable interest to the life sciences.

Gradient surfaces are those which have a gradual, spatiotemporal variation of one or more chemical, physical, or topographical properties. A variety of methods have been reported for the fabrication of surface gradients[17−19] including UV-initiated free-radical polymerization[8] and grafting,[20] corona discharge,[21−23]

*E-mail: ben.muir@csiro.au.

(1) Zelzer, M.; Majani, R.; Bradley, J. W.; Rose, F.; Davies, M. C.; Alexander, M. R. *Biomaterials* **2008**, *29*(2), 172–184.
(2) Busscher, H. J.; Ruardy, T. G.; Van der Mei, H. C.; Schakenraad, J. M. *Surf. Sci. Rep.* **1997**, *29*(1), 3–30.
(3) Parry, K. L.; Shard, A. G.; Short, R. D.; White, R. G.; Whittle, J. D.; Wright, A. *Surf. Interface Anal.* **2006**, *38*(11), 1497–1504.
(4) Shin, Y. N.; Kim, B. S.; Ahn, H. H.; Lee, J. H.; Kim, K. S.; Lee, J. Y.; Kim, M. S.; Khang, G.; Lee, H. B. *Appl. Surf. Sci.* **2008**, *255*(2), 293–296.
(5) Yang, J.; Rose, F., R. A. J.; Gadegaard, N.; Morgan, A. R. *Adv. Mater.* **2009**, *21*(3), 300–304.
(6) Lee, J. H.; Lee, H. B. *J. Biomed. Mater. Res.* **1998**, *41*(2), 304–311.
(7) Blondiaux, N.; Morgenthaler, S.; Pugin, R.; Spencer, N. D.; Liley, M. *Appl. Surf. Sci.* **2008**, *254*(21), 6820–6825.
(8) Ekblad, T.; Andersson, O.; Tai, F. I.; Edeith, T.; Liedberg, B. *Langmuir* **2009**, *25*(6), 3755–3762.
(9) Fischer, D. A.; Efimenko, K.; Bhat, R. R.; Sambasivan, S.; Genzer, J. *Macromol. Rapid Commun.* **2004**, *25*(1), 141–149.
(10) Genzer, J.; Fischer, D. A.; Efimenko, K. *Appl. Phys. Lett.* **2003**, *82*(2), 266–268.
(11) Wong, J. Y.; Velasco, A.; Rajagopalan, P.; Pham, Q. *Langmuir* **2003**, *19*(5), 1908–1913.
(12) Pelham, R. J., Jr; Wang, Y. L. *Proc. Natl. Acad. Sci. U.S.A.* **1997**, *94*(25), 13661–13665.
(13) Smith, J. T.; Tomfohr, J. K.; Wells, M. C.; Beebe, T. P.; Kepler, T. B.; Reichert, W. M. *Langmuir* **2004**, *20*(19), 8279.
(14) Singh, M.; Berkland, C.; Detamore, M. S. *Tissue Eng. Part B: Rev.* **2008**, *14*(4), 341–366.
(15) Vasilev, K.; Mierczynska, A.; Hook, A. L.; Chan, J.; Voelcker, N. H.; Short, R. D. *Biomaterials* **2009**, *31*(3), 392–397.
(16) DeLong, S. A.; Gobin, A. S.; West, J. L. *J. Controlled Release* **2005**, *109*(1), 139–148.
(17) Morgenthaler, S.; Zink, C.; Spencer, N. D. *Soft Matter* **2008**, *4*(3), 419–434.
(18) Genzer, J.; Bhat, R. R. *Langmuir* **2008**, *24*(6), 2294.
(19) Bhat, R. R.; Tomlinson, M. R.; Wu, T.; Genzer, J. Surface-Grafted Polymer Gradients: Formation, Characterization, and Applications. Surface-Initiated Polymerization II, Springer-Verlag: Berlin, 2006; Vol. *198*, pp 51−124.
(20) Li, B.; Ma, Y.; Wang, S.; Moran, P. M. *Biomaterials* **2005**, *26*(24), 4956–4963.
(21) Iwasaki, Y.; Ishihara, K.; Nakabayashi, N.; Khang, G.; Jeon, J. H.; Lee, J. W.; Lee, H. B. *J. Biomater. Sci., Polym. Ed.* **1998**, *9*(8), 801–816.
(22) Lee, S. J.; Khang, G.; Lee, Y. M.; Lee, H. B. *J. Colloid Interface Sci.* **2003**, *259*(2), 228–235.
(23) Lee, T. G.; Shon, H. K.; Kim, M. S.; Lee, H. B.; Moon, D. W. *Appl. Surf. Sci.* **2006**, *252*(19), 6754–6756.

corona-induced graft copolymerisation,[24] diffusion techniques,[13,25] adsorption,[26] and plasma copolymerization.[27] The use of radio frequency plasma polymerization (RFpp) has also been reported for gradient generation[1,28−30] and to date has required the use of a moving sample stage or shutter. Our one-step method of gradient generation uses RFpp without the need for any moving components.

Gradient surfaces have been used to study the interaction and function of both cells and biomolecules, such as proteins. Wettability gradients formed by treating various polymeric substrates such as polyethylene[31] and polylactide-glycolide[32] films in air with corona discharge from a knife-type electrode have been used to investigate the effect of wettability on protein adsorption,[33,34] platelet adhesion[6] and cell adhesion, spreading and growth.[32,34,35] Chemical gradients presenting various chemical functionalities have also been used to study many biological interactions in vitro. Robinson et al.[30] used plasma polymerization of octadiene and allylamine monomers to form compositional gradients that enable the formation of immobilized, functional heparin gradients. Similarly, Zelzer et al.[1] formed chemical gradients using plasma polymerization of hexane and allylamine to investigate the optimal surface chemistry and wettability for the attachment and differentiation of fibroblasts. A number of researchers have also used surface chemical gradients as a high throughput approach to screening and identifying the critical parameters involved in the interaction of, or resistance to, various proteins and platelets.[36,37]

The use of poly(ethylene glycol) based materials to impart protein resistance is well described and the use of PEG-based gradients provides an ideal surface to interrogate the important chemical and physical characteristics that impart PEG's protein resistant nature. The mechanisms of PEG's protein resistance have been extensively investigated[38,39] and two of the most well regarded explanations include "steric stabilization"[40,41] and the "water barrier" theories. Latour[42] recently encompassed these theories into a thermodynamic approach, where he suggests that the enthalpic (favored H-bonding of the tethered chains to water molecules rather than to the functional groups on the proteins) and entropic effects resulting from protein adsorption cause a net increase in the free energy of the system upon protein adsorption. However, this theory assumes the presence of PEG surfaces with long flexible surface-tethered chains having both a low packing density (to allow a high mobility) yet providing full coverage on the surface. These assumptions are not particularly relevant, however, to the highly cross-linked PEG-like surfaces produced from plasma polymerization described in this study.

We have produced 1D surface bound PEG-like chemical gradients in one step, using continuous wave radio frequency glow discharge (rfgd) plasma polymerization of diethylene glycol dimethyl ether (DG). Using a knife edge upper electrode, a non-uniform plasma glow discharge was generated around the upper electrode resulting in the deposition of a chemical gradient on substrates placed directly underneath the plasma glow. The chemistry across the DGpp gradients was analyzed using grazing-incidence FTIR (gi-FTIR) microspectroscopy to provide a chemical map of the bulk chemistry across the gradients. X-ray photoelectron spectroscopy (XPS) and near edge X-ray absorption fine structure (NEXAFS) provided complementary surface sensitive chemical analysis of these gradients. NEXAFS has been shown to be an excellent combinatorial tool for studying surface bound gradients due to its ability to analyze both surface chemistry and molecular orientation.[9,10] The adsorption of three model proteins (bovine serum albumin (BSA), lysozyme (Lys), and γ-globulin (IgG) was measured across the gradients, and these demonstrated marked variability in their ability to resist protein adsorption that correlated with changes in surface chemistry.

Materials and Methods

Substrate Preparation. DGpp gradients were deposited onto ultraflat single crystal silicon wafers (⟨100⟩, 1 × 3 cm, 0.5 mm thick, MMRC P/L), cleaned by ultrasonication in a 1% RBS-35 surfactant (Pierce) in (2% ethanol in Milli-Q) for 1 h. Substrates were then rinsed multiple times in Milli-Q water before being dried in a high-pressure stream of high purity nitrogen. Indium tin oxide coated aluminosilicate glass (Delta Technologies, Corning 1737, CB-50IN) was used for the giFTIR analysis to provide a reflective surface, and was cleaned as described above.

Plasma Polymerization. Radio frequency glow discharge plasma polymerization was used to deposit PEG-like gradient films in a custom-built plasma reactor. The reactor consists of a cylindrical glass chamber (height of 35 cm and diameter of 17 cm) and is fitted with two capacatively coupled electrodes. The top electrode (a razor) was connected to a RF power supply (125 kHz) and lowered to sit ∼1 mm above the substrate, while the bottom electrode (diameter = 14 cm) was grounded (see Supporting Information). The monomer, diethylene glycol dimethyl ether, often referred to as "diglyme" (DG; BDH, 99% purity) was fed into the reactor from a round-bottom flask attached to a stainless steel line and a manual valve to control the flow. Substrates were placed on the lower electrode, and a rotary pump was used to evacuate the chamber. The DG vapors were fed into the chamber at a starting pressure of 20 Pa, and a continuous RF field was generated between the electrodes for a deposition time of 180 s. Gradients were deposited at two different load powers, 5 and 30 W.

Profilometry. Film thickness across the gradient was measured using a Veeco Dektak 6 M stylus profilometer. Briefly, the stylus (diameter 12.5 μm) force was set to 10 mg across a distance of 1000 μm over 10 s. A thin line of the DGpp gradient was removed in the direction of the gradient by scratching the surface with a sharp needle to expose the silicon substrate. Measurements were then taken over the scratch across the gradient at 1 mm interval to assess film thickness.

(24) Jeong, B. J.; Lee, J. H.; Lee, H. B. *J. Colloid. Interf. Sci.* **1996**, *178*(2), 757–763.
(25) Liedberg, B.; Wirde, M.; Tao, Y. T.; Tengvall, P.; Gelius, U. *Langmuir* **1997**, *13*(20), 5329–5334.
(26) Morgenthaler, S.; Lee, S.; Zürcher, S.; Spencer, N. D. *Langmuir* **2003**, *19*(25), 10459–10462.
(27) Vasilev, K.; Mierczynsk, A.; Hook, A.; Chan, J.; Voelcker, N. H.; Short, R, D. *Biomaterials* **2010**, *31*, 392–397.
(28) Wells, N.; Baxter, M. A.; Turnbull, J. E.; Murray, P.; Edgar, D.; Parry, K. L.; Steele, D. A.; Short, R. D. *Biomaterials* **2009**, *30*(6), 1066–1070.
(29) Ogumi, Z.; Abe, T.; Nakamura, S.; Inaba, M. *Solid State Ionics* **1999**, *121*(1), 289–293.
(30) Robinson, D. E.; Marson, A.; Short, R. D.; Buttle, D. J.; Day, A. J.; Parry, K. L.; Wiles, M.; Highfield, P.; Mistry, A.; Whittle, J. D. *Adv. Mater.* **2008**, *20*(6), 1166–1169.
(31) Lee, J. H.; Lee, H. B. *J. Biomater. Sci., Polym. Ed.* **1993**, *4*(5), 467–481.
(32) Khang, G.; Rhee, J. M.; Lee, J. H.; Lee, I.; Lee, H. B. *Kor. Polym. J.* **2000**, *8*(6), 276–284.
(33) Spijker, H. T.; Bos, R.; van Oeveren, W.; de Vries, J.; Busscher, H. J. *Colloids Surf., B* **1999**, *15*(1), 89–97.
(34) Xu, L. C.; Siedlecki, C. A. *Biomaterials* **2007**, *28*(22), 3273–3283.
(35) Li, B.; Ma, Y.; Wang, S.; Moran, P. M. *Biomaterials* **2005**, *26*(13), 1487–1495.
(36) Spijker, H. T.; Bos, R.; Busscher, H. J.; van Kooten, T. G.; van Oeveren, W. *Biomaterials* **2002**, *23*(3), 757–766.
(37) Corum, L. E.; Hlady, V. *Biomaterials* **2009**, *31*(12), 3148–3155.
(38) Sheth, S. R.; Leckband, D. *Proc. Natl. Acad. Sci. U.S.A.* **1997**, *94*(16), 8399–8404.
(39) Szleifer, I. *Physica A* **1997**, *244*(1), 370–388.
(40) Kingshott, P.; Thissen, H.; Griesser, H. J. *Biomaterials* **2002**, *23*(9), 2043–2056.
(41) Li, L.; Chen, S.; Zheng, J.; Ratner, B. D.; Jiang, S. *J. Phys. Chem. B* **2005**, *109*(7), 2934–2941.
(42) Latour, R. A. *J. Biomed. Mater. Res. Part A* **2006**, *78A*(4), 843–854.

Grazing Incidence FTIR Microspectroscopy. Chemical maps across the DGpp gradients were measured using a FTIR microscope at the infrared beamline at the Australian Synchrotron. A Bruker Vertex 80v FTIR spectrometer with a KBr beam splitter and vacuum windows is coupled to a Bruker Hyperion 2000 IR microscope (Bruker Optik GmbH, Ettlingen, Germany) which is equipped with a liquid nitrogen cooled single point MCT detector and motorized sample stage which allows for point by point raster scanning of the sample. Spectra were collected in grazing incidence mode using a Bruker Grazing Angle Objective (GAO) at 15× magnification. An IR polarizer was used to ensure the perpendicular polarization vector of the incident radiation to the sample surface. All data were collected using the Bruker Opus software version 6.5 with the video mapping package used for generation of two-dimensional grazing angle absorbance maps. FTIR spectra were acquired at a spectral resolution of 6.0 cm^{-1} with 256 scans coadded and normalized to the alkane stretch (~2850 to 3000 cm^{-1}) to compensate for any thickness effects across the gradient. A 20 × 20 μm aperture was used at step intervals of 250 μm across the length of the gradients to build a surface plot showing the 1D spatial variation of the FTIR spectra.

X-ray Photoelectron Spectroscopy (XPS). To investigate the chemical composition of the DGpp films, XPS analysis was performed using an AXIS HSi spectrometer (Kratos Analytical Ltd., Manchester, U.K.) equipped with a monochromated Al Kα X-ray source at a power of 144 W (12 mA, 12 kV). A hemispherical analyzer was used, operating in the fixed analyzer transmission mode with a standard aperture (1.0 × 0.5 mm). Charging of the samples during irradiation was compensated for by the internal flood gun, coupled with a magnetic immersion lens. The pressure in the main vacuum chamber during analysis was typically 5×10^{-6} Pa.

Survey spectra were acquired at a pass energy of 320 eV to identify the elements present in the DGpp films. The atomic concentrations were calculated using integral peak intensities and the sensitivity factors supplied by the manufacturer. High-resolution C 1s spectra were also obtained and quantified using a minimization algorithm in order to calculate optimized curvefits and determine the relative contributions from specified functional groups.

Five peak components (mixed guassian/Lorentzian model functions) were used. Component C1 at the lowest binding energy (BE) was assigned to aliphatic hydrocarbons (neutral carbon) and the corresponding BE set accordingly to 285 eV.[43] A second component at a slightly higher BE was included to account for all C 1s photoelectrons that underwent a secondary BE shift. Component C3 (286.3−286.6 eV) represents C−O based groups (e.g., ethers and alcohols), C4 (287.9−288.2 eV) accounts for all C═O based functional groups (e.g., aldehydes and ketones) and C5 (288.9−289.3 eV) accounts for O−C═O based groups (e.g., acids or esters). These components were applied to the analysis of the DGpp gradients prior to protein adsorption.

Near Edge X-ray Adsorption Fine Structure (NEXAFS) spectroscopy. NEXAFS spectroscopy was performed at the Australian Synchrotron on the soft X-ray beamline (SXR, 14-ID). Samples were loaded into a UHV chamber, where a vacuum of 2×10^{-8} kPa was maintained. The beamline is equipped with an Apple II undulator, which was set to produce horizontally polarized light that is then passed through a monochromator (Peterson plane grating, 1200 lines mm^{-1}). The photon flux on the beamline was 2.7×10^{11} photons/s/200 mA, and the beam spot size on the sample was approximately 0.6 × 0.6 mm. Spectra were acquired (with the beam at 90° wrt the sample surface) for both the C (270−320 eV) and O (520−560 eV) K-edge in partial electron yield (PEY) mode. Simultaneously, drain current spectra were collected from an Au mesh placed in front of the sample to allow for normalization of the synchrotron beam energy between scans. A retarding potential of −100 and −400 eV for the C and O scans, respectively, was applied to the entrance of the detector to eliminate any contributions from lower energy electrons. Multiple spectra on the same spot retained the same spectral features, indicating that the films are not subject to radiation damage. To account for contributions to the O 1s and C 1s spectra from internal contamination from the beamline itself, a clean sputtered Au foil was measured as a reference. Spectra were then normalized according to the method discussed by Watts et al.[44] Energy alignment of the carbon binding energy scale was achieved using the C 1s → π^* resonance, measured with a pyrolytic graphite sample and was fixed to the value of 285.4 eV. A Vanadium oxide (V_2O_3) standard was used to normalize the binding energy of the oxygen spectra from its O L_{III}-edge transition energy and was fixed to the value of 517.5 eV. A MatLab based curve fitting program, Whooshka was used to curve-fit the NEXAFS spectra, where a series of Gaussian peaks were assigned to fit the resonance features along with a step edge.

Surface Derivatisation. Using the method described by Shard et al.,[45] surface derivatization of the hydroxyl groups across the DGpp gradient films was performed using gas phase reaction with trifluoroacetic anhydride (TFAA). Briefly, a small volume TFAA was placed in a vial and the gradient film attached to the lid of the vial. The sample was gently agitated for approximately 30 s and left for approximately 1 h for the reaction to take place. Samples were then analyzed for their atomic composition and using the equation below, the concentration of hydroxyl groups was calculated.

$$X_{C\text{-}OH} = 1/(3(I_c S_f / I_f S_c)\text{-}2) \quad (1)$$

where I is the intensity (of C and F) and S is the sensitivity factor (of C and F).

To determine to what degree and in what manner the proteins are bound to the gradient surfaces, the grafting capability of the copolymer poly(L-lysine)-poly(ethylene glycol) (PLL-*g*-PEG) with the primary amine (1°) functionalities of the protein was assessed. Two mechanisms of reaction are possible, namely covalent or electrostatic. Covalent bonding involves attachment of the 1° amines via either aldehyde or ketone groups; whereas electrostatic interactions react via residual acid functionalities within the gradient surfaces. Samples were incubated overnight at room temperature with 1 mg/mL PLL-*g*-PEG solutions in water (pH 5) and were rinsed with Milli-Q water prior to analysis of the N content using XPS.

Protein Adsorption. To assess the relative adsorption of various proteins across the DGpp gradients, fresh samples were incubated in solutions of bovine serum albumin, Lys, and γ-globulins proteins (1 mg/mL in PBS, pH 7.4 for 1 h). Samples were then thoroughly rinsed with Milli-Q water before being blown dry with a high-velocity, ultra pure nitrogen stream. Samples were then analyzed using XPS where protein adsorption was indicated by the presence of elemental N on the DGpp gradient surface.

(43) Watts, J. F. *Surf. Interface Anal.* **1993**, *20*(3), 267.

(44) Watts, B.; Thomsen, L.; Dastoor, P. C. *J. Electron. Spectrosc.* **2006**, *151*(2), 105–120.

(45) Shard, A. G.; Whittle, J. D.; Beck, A. J.; Brookes, P. N.; Bullett, N. A.; Talib, R. A.; Mistry, A.; Barton, D.; McArthur, S. L. *J. Phys. Chem. B* **2004**, *108*(33), 12472–12480.

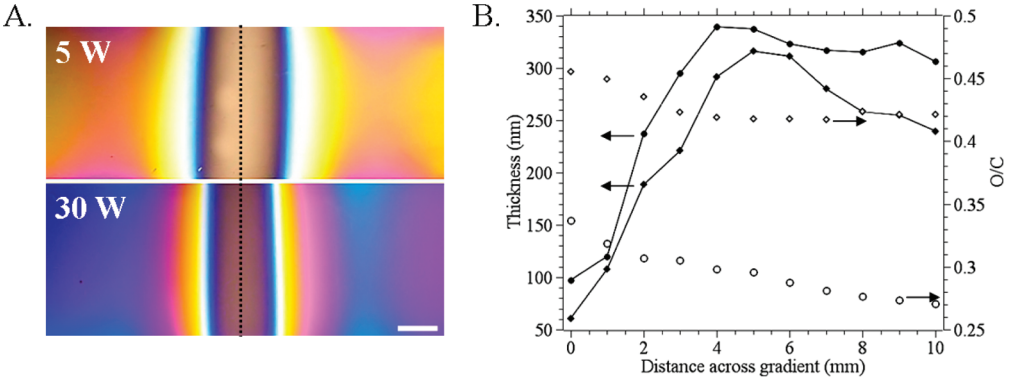

Figure 1. A. Photographic images of DGpp gradients deposited on Si at 5 and 30 W load powers. The color change across the gradient films is indicative of changing film thickness with distance. The broken vertical line indicates the projected position of the knife-edge electrode during deposition. B. Film thickness (dark symbols, lines are a guide for the eye) and O/C elemental ratio (hollow symbols) plotted across the 5 (♦) and 30W (●) DGpp gradients as a function of distance. Arrows indicate to which axis the data relates.

Results and Discussion

Plasma deposition. In this work, PEG like gradient plasma polymer (pp) thin films were deposited via radio frequency glow discharge plasma polymerization of diethylene glycol dimethyl ether (DG) at two different load powers, 5 and 30 W. Using a knife edge upper electrode within the plasma reactor, a nonuniform plasma glow discharge was created around the upper electrode (razor), resulting in DGpp gradient films with a systematic variation in both their surface chemistry and thickness. We hypothesize that the top razor electrode results in the formation of a nonuniform plasma sheath directly beneath it. This results in a spatial variation of the monomer fragmentation rate and plasma polymer deposition conditions extending outward from the knife edge electrode. Further discussion of the plasma physical processes (with regards to magnetic field variation, plasma bulk, and sheath potentials etc.) occurring during the glow discharge is beyond the scope of this work. Photographic images of the DGpp gradients (produced at an electrode separation distance of 1 mm) deposited on a Si substrate are presented in Figure 1A. The color changes occurring across the DGpp coated substrate are indicative of the variation in film thickness. We have noted that as the separation distance between the razor and bottom earthed electrode is increased from 1 to 4 mm, the slope and size of the gradient produced dramatically decreases. At electrode separation distances over 4 mm, the gradient completely disappears. For this reason, all analysis was performed on gradients produced at a separation distance of 1 mm.

Profilometry measurements were performed across the DGpp gradients to measure film thickness (Figure 1B). The central region of the DGpp gradients, deposited directly under the knife edge electrode will be referred to as '0 mm' throughout this paper. The 5W DGpp gradient showed an increasing film thickness from 0 mm to a distance of 5 mm and then a systematic decrease when measured out to 10 mm. Similarly, the film thickness across the 30W gradient increased between 0 and 4 mm and then decreased out to 10 mm but produced thicker gradients in comparison to the 5W coatings, indicating a faster film deposition rate at higher load powers as would be expected. XPS elemental analysis of the DGpp films showed the presence of both oxygen and carbon, with the oxygen content remaining highest at the center of the gradients (data not shown). A similar trend was observed for both the 5 and 30 W gradient films; however films deposited at 30 W retained lower levels of oxygen. Analysis of the O/C atomic ratio (Figure 1B) across the gradients ranged from 0.46 (at 0 mm) to 0.42 (10 mm) in the case of the 5 W films and from 0.33 (0 mm) to 0.26 (10 mm) in the case of the 30 W film. The O/C ratio of the starting diglyme monomer is 0.5.

giFTIR Microspectroscopy. The variation of the bulk plasma polymer thin film gradient chemistries produced during the rfgd of DG at load powers of 5 and 30 W was investigated using gi-FTIR microspectroscopy with a synchrotron radiation source. FTIR spectra from 20×20 μm sample regions were acquired to 15 mm either side of the gradient center (0 mm), at a spatial distance of 250 μm intervals across the gradients. Figure 2 presents 3-dimensional FTIR spectral plots taken across the 5 and 30 W gradient films. Surface plots of the ether (COC), carbonyl (C═O) and hydroxyl (OH) stretches as a ratio to the hydrocarbon (CH) stretch are also reported in the Supporting Information. The dominant peak observed in the spectra was the ether stretch at ~1052 cm^{-1}. It is possible that some contribution to this stretch may also be from residual ester groups in the gradient films. It was shown that the gradients retain the greatest monomer-like functionality (high ether content) in the central region (0 mm) of the gradient that is deposited directly underneath the knife edge electrode. The formation of new chemical species after plasma polymer deposition is well documented and generally occurs as a result of post oxidation reactions and scission of the starting monomer or oligomer species in the plasma glow discharge. A systematic decrease in the absorbance of the ether stretch (COC) extending out from the central region of the gradient was observed, which was even more pronounced in the 30 W DGpp gradient. The carbonyl stretch at ~1735 cm^{-1} showed the opposite trend to the ether stretch with lower carbonyl intensity observed at the center of the gradients where fragmentation of the monomer species appears to be occurring to a lesser extent. The spectra, normalized to the alkane stretch (~2850−3000 cm^{-1}, which incorporates the stretch vibrations from both CH_2CH_2 and CH_3 groups) indicate that very low levels of carbonyl containing species are present in the center of the 5 W gradient, although compared to the 30 W film it has a much greater concentration of ether functionality present. It is difficult to assign the exact origin of the carbonyl species in this work due to the closeness of acid, ester, aldehyde and ketone stretches in this region and the inherently broader nature of the DGpp films spectral peaks in comparison to small molecule FTIR spectra. In the gradient deposited at the 30 W plasma load power, higher levels of carbonyl functionality were observed but again remained lowest in the center of the gradient at 0 mm. Analysis of the hydroxyl stretch (~3450 cm^{-1}) showed a variation in intensity across the 5 W gradient with lower levels seen at the central region,

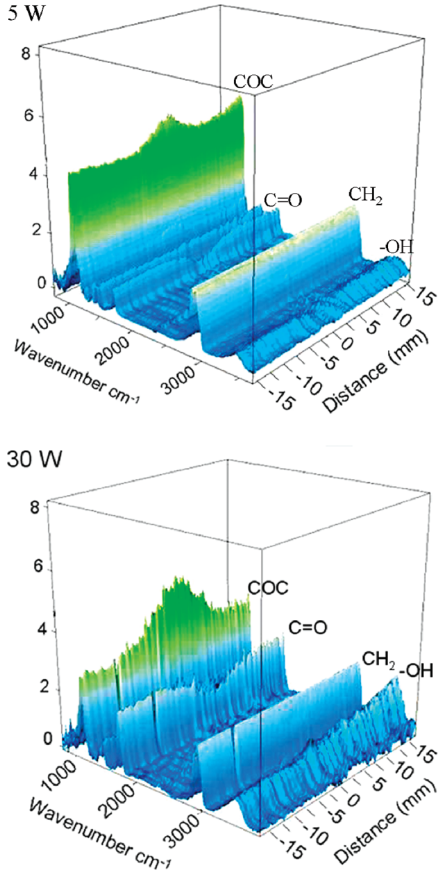

Figure 2. 3D grazing incidence synchrotron source FTIR spectroscopy surface plots measured along the 5 and 30 W DGpp gradients. The spectra show the major functional groups observed are ether, carbonyl and hydroxyl groups (approx 1052, 1735, and 3450 cm^{-1}, respectively). To avoid thickness effects contributing to the relative absorption of various functionalities, all peaks measured were relative to the normalized alkane stretch (~2850−3000 cm^{-1}).

however no systematic trend was observed across the 5 W gradient. Another point of interest to note from the FTIR spectra is the absence of an alkene stretch (~1621 cm^{-1}), indicating that no detectable concentration of C═C bonds was observed using the gi-FTIR technique. The absence of the alkene stretch absorption from FTIR analysis has also recently been reported by Cheng et al.[46] in an FTIR study of pulsed plasma deposited bulk chemical DGpp thin films.

X-ray Photoelectron Spectroscopy. High resolution C 1s XPS analyses were performed across the two DGpp gradients to characterize their surface chemistry and were compared to the bulk functional group analysis generated from the gi-FTIR microspectroscopy data. Analysis of the C 1s spectra revealed four main contributing chemical components including C−C and C−H (hydrocarbon), C−OR (ether and alcohol), C═O (ketone and aldehyde), and COOR (carboxylic acid and ester). Figure 3 presents curve fitted component data as a percentage of each C1s component discussed versus distance from the center of the 5 and 30 W gradient films. The central region of both the 5 and 30 W gradients, retained the highest concentration of COR groups (~ 286.6 eV) indicating a higher retention of the monomer ether functionality. A systematic decrease in the ether (C−OR) functionality from the center and across the gradient was observed, consistent with the gi-FTIR analysis of the bulk DGpp gradient film chemistries. Spectroscopic analysis shows that the ether content of the 5 W gradient film changes more dramatically at its surface (from XPS analysis) than its bulk (FTIR analysis). The opposite is true for the 30 W film with this gradient showing a stronger bulk chemical, rather than surface chemical variation across its length. C 1s analysis also revealed that the C−C/C−H (~285 eV), C═O (288 eV), and COOR (289.1 eV) functionalities were lowest in the center (0 mm) and increased across the gradients. Gradients deposited at a 5 W load power retained more monomer-like functionality compared with the 30 W gradient, with higher concentrations of C-OR groups and lower concentrations of the C−C/C-H, C═O and COOR functionalities. The 5W gradient film yielded C-OR concentrations ranging from 79% at the center (0 mm) to 57% at 10 mm, compared with 46% (0 mm) to 25% (10 mm) for the 30 W films. The loss of COR functional groups corresponded with an increase in hydrocarbon species and in the 30 W gradient film, the concentration of COR units in the central region is equivalent to the concentration of hydrocarbon (CC/CH) units. There was a small variation in the concentration of C═O and COOR functionalities between gradients; however aldehyde and ketone C═O groups were present at a higher concentration in both gradients compared to the acidic and ester (COOR) groups. The central region of each gradient also had lower levels of C═O and COOR species.

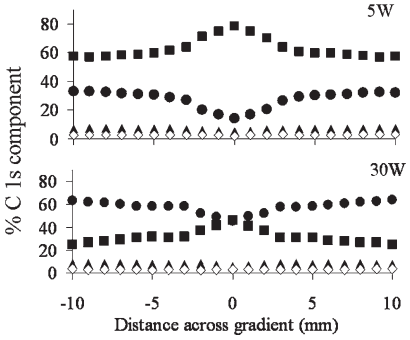

Figure 3. XPS C1s curve fitted component data presented as percentage C1s component vs distance from the center of the 5 and 30 W gradient films. Fitted components are C−C, C−H (■), C−O (●), C═O (▲), and O−C═O (◊), and percentages are relative to total carbon.

Bretagnol et al.[47] reported on DGpp films deposited via pulsed rfgd plasma polymerization yielding surfaces composed of 70−74% COR functionalities at a load power of 1 W. While using continuous wave rfgd plasma polymerization at a load power of 15 W, they report a final film COR content of just 40%. This finding is interesting as it demonstrates that the geometry of the electrodes used in plasma polymer film deposition can have a significant influence over the final film chemistry and that using a continuous rfgd plasma polymerization process we are able to obtain comparable results to that of a pulsed plasma technique. Similarly, Cheng et al.[46] recently reported the deposition of DG vapors using pulsed rfgd plasma polymeriztaion where the highest COR content was reported to be 72% at a load power of 1 W. The 5 W gradients deposited for this study yielded COR contents of > 70% within 2 mm either side of the gradient center, decreasing to 57% at a distance of 10 mm. Our generic approach therefore provides a one step deposition method for generating a gradient

(46) Cheng, Q.; Komvopoulos, K. *J. Phys. Chem. C* **2009**, *113*(1), 213–219.

(47) Brétagnol, F.; Lejeune, M.; Papadopoulou-Bouraoui, A.; Hasiwa, M.; Rauscher, H.; Ceccone, G.; Colpo, P.; Rossi, F. *Acta Biomater.* **2006**, *2*(2), 165–172.

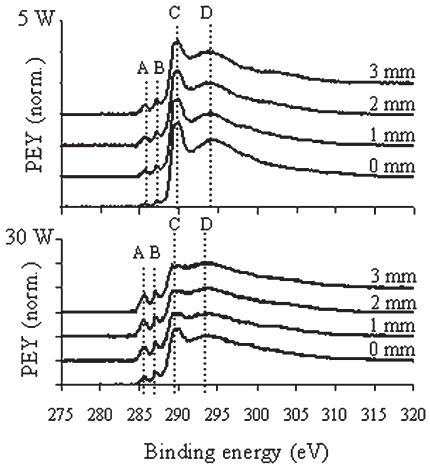

Figure 4. C 1s K-edge NEXAFS spectra plotted across the 5 and 30 W DGpp gradient films between 0 and 3 mm. (A, C 1s $\rightarrow \pi^*_{(C=O)}$; B, C 1s $\rightarrow \sigma^*_{(C-H)}$; C, C 1s $\rightarrow \sigma^*_{(C-O)}$; D, C 1s $\rightarrow \sigma^*_{(C-C;C-O)}$). The central region of each gradient and films deposited at lower load power retained lower C=O and CH species, which systematically increase outward.

composition of COR functionalities and a high throughput platform for studying the chemical nature of these films. Previous studies of these types of plasma polymer films have necessitated the deposition of multiple samples to investigate their protein resistance and surface chemistries.

NEXAFS Spectroscopy. To further analyze the chemistry across the DGpp gradients, and detect any the orientation of terminal chains across the DGpp gradients, a C and O K-edge PEY NEXAFS spectroscopy study was performed. Analysis of the C 1s spectra revealed four main resonance features (Figure 4) including C 1s $\rightarrow \pi^*_{(C=O)}$ excitation at ~285.7 eV (A), C 1s $\rightarrow \sigma^*_{(C-H)}$ at ~287.3 eV (B), C 1s $\rightarrow \sigma^*_{(C-O)}$ at ~289.9 eV (C), and a broader C 1s $\rightarrow \sigma^*_{(C-C;C-O)}$ feature at ~294.4 eV (D) . Due to the multiphoton resonance absorptions and the broader nature of the higher energy σ-bonded species, only the two lower energy features (C=O π^* and C−H σ^*) will be compared and discussed. To quantify and compare the relative concentration of these various bonded species, spectral features were integrated using a curve fitting procedure (discussed in the Methods section) and the area compared across the gradients and between the gradients deposited at the two load powers (see Supporting Information for example curve fits and O K-edge NEXAFS results and analysis).

Results presenting the integrated area plots of the C=O π^* and C−H σ^* resonance features from the C 1s K-edge spectra, plotted across the two DGpp gradients (5 and 30 W) 3 mm either side of the center (0 mm) show that the center of each gradient had lower concentrations of unsaturation (C=O) and hydrocarbon species (Supporting Information), systematically increasing outward. This is consistent with the data obtained from XPS and gi-FTIR analysis. Higher levels of unsaturation and hydrocarbon species were introduced into the gradients as the load power was increased during plasma deposition. This is also consistent with information reported by Swaraj et al.,[48] who analyzed pulsed-plasma deposited ethylene samples using NEXAFS and reported that films deposited under higher load powers contained higher levels of unsaturation.

The use of NEXAFS as a tool for the analysis of plasma polymers[45,49−51] and PEG-like films is in its infancy. Zwahlen et al.[52] reported a C and O K-edge NEXAFS analysis of oligo-(ethylene glycol) (OEG) terminated alkanethiol SAMs on gold and their reported peak assignments are consistent with those reported in Figures 4. They investigated the degree of order in OEG SAMs films made from different length oligomers and found that only shorter length oligomers showed a weak angular dependence. Due to the fragmentation, polymerization and cross-linking process that occur during plasma polymerization, both the C 1s and O 1s NEXAFS spectra obtained for the DGpp gradients have the additional C=O π^* resonance features when compared to OEG SAMs. A number of researchers have used NEXAFS spectroscopy as part of a combinatorial approach to the analysis of surface gradients by mapping the surface chemistry as well as varying the polarization of the light source, in order to detect any preferred orientation of the surface bound materials.[9,10] We performed similar experiments to test for any possible orientation of polymer chains in the DGpp film gradients analyzing C and O K-edge NEXAFS spectra using both horizontally and vertically polarized light. No difference was seen in spectra obtained from horizontally or vertically polarized light, indicating no preferred orientation, presumably due to the amorphous and cross-linked nature of the plasma polymer (dry) films in vacuum when analyzed.

Surface Derivatisation. Spectroscopic analysis of the DGpp gradient films revealed contributions from a number of chemical functionalities. To further deduce specific chemical functionalities that may have been present in the films such as residual hydroxyl, aldehyde/ketone and acid groups, a chemical derivatization study was performed on the 5 and 30 W DGpp gradient films. Derivatisation of surface functionalities with reactive fluorinated compounds has been well reported and discussed[53,54] in the literature for use as XPS markers, since XPS cannot, for example, differentiate between certain chemical functionalities such as hydroxyls and ethers in the COR C1s component. By using a gas phase reaction between any potential surface hydroxyl species along the DGpp gradients with trifluoroacetic anhydride (TFAA),[55] it is possible to deduce the concentration (eq 1) of residual hydroxyl groups on the surface and therefore the actual concentration of surface ether groups. It is important to note, however that surface derivatization might only access the reactive groups at the top surface whereas the COR XPS signal XPS signal originates from a 5−10 nm thick surface layer. Figure 5A presents the F/C plots from quantified XPS survey spectra across the 5 and 30W DGpp gradient films after derivatization with TFAA. Interestingly the two films show opposite trends in terms of their hydroxyl content with distance from the center of the film. Results indicate a higher total surface concentration of hydroxyl functionalities across the 5W DGpp gradient with a slightly lower level in the center (0 mm) of the gradient. The 30 W DGpp gradient displayed a high concentration of hydroxyl species in the center of the gradient which systematically decreased moving outward across the gradient. Using this data the normalized surface ether

(48) Swaraj, S.; Oran, U.; Lippitz, A.; Schulze, R. D.; Friedrich, J. F.; Unger, W. E. S. *Plasma. Process. Polym.* **2005**, *2*(4), 310–318.
(49) Kim, Y.; Kim, K. J.; Lee, Y. *Surf. Coat. Technol.* **2009**, *203*(20), 3129–3135.
(50) Oran, U.; Swaraj, S.; Lippitz, A.; Unger, W. E. S. *Plasma. Process. Polym.* **2006**, *3*(3), 288–298.
(51) Friedrich, J. F.; Geng, S.; Unger, W.; Lippitz, A.; Erdmann, J.; Gorsler, H. V.; Wöll, C.; Schertel, A.; Bierbaum, K. *Surf. Coat. Technol.* **1995**, *74−75*(Part 2), 664–669.
(52) Zwahlen, M.; Herrwerth, S.; Eck, W.; Grunze, M.; Hahner, G. *Langmuir* **2003**, *19*(22), 9305–9310.
(53) Buchholz, V.; Adler, P.; Backer, M.; Hölle, W.; Simon, A.; Wegner, G. *Langmuir* **1997**, *13*(12), 3206–3209.
(54) Chilkoti, A.; Castner, D. G.; Ratner, B. D.; Briggs, D. *J. Vac. Sci. Technol. A* **1990**, *8*(3), 2274–2282.
(55) Friedrich, J.; Unger, W.; Lippitz, A.; Geng, S.; Koprinarov, I.; Kühn, G.; Weidner, S. *Surf. Coat. Technol.* **1998**, *98*(1), 1132–1141.

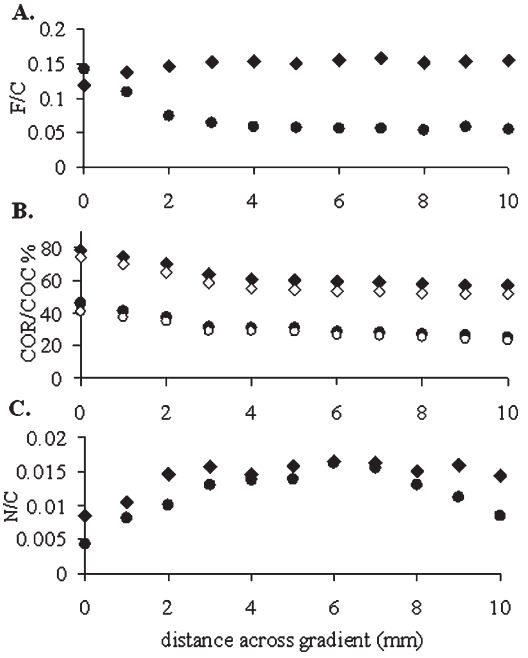

Figure 5. XPS elemental and chemical species analysis from C 1s curve fits and survey spectra of the 5 and 30 W gradient DGpp thin films. A. The resulting F/C values plotted across the 5 (♦) and 30 W (●) gradient films after gas phase derivatization of surface hydroxyl groups using TFAA. B. The "actual" surface ether content was calculated across the gradients before and after chemical derivatization of surface hydroxyl groups from the COR component of the C 1s curve-fit (hollow symbols represent the normalized ether content after surface derivatization). C. The resultant N/C values plotted across the 5 and 30 W gradient films after incubation with PLL-*g*-PEG.

concentration was calculated across the 5 and 30 W gradients and Figure 5B shows the ether concentration plotted both before and after subtracting the hydroxyl contributions (to the COR C 1s component). The actual ether concentration across the 5 W gradients was then calculated ranging from 74% (0 mm) to 51% (10 mm) while the 30 W ranged from 41% (0 mm) to 23% (10 mm). Although the 5 W DGpp gradient films may contain more surface hydroxyl species, overall it has a far greater concentration of "monomer like" ether functionalities retained in the film when compared to the 30 W gradient films. This result highlights the fact that as the plasma power is increased a greater number of oxygen containing chemical functionalities are being generated during and possibly after thin film deposition, within the surface and bulk of the DGpp gradient coatings.

Spectroscopic analysis of the films alluded to possible reactive chemical functionalities such as aldehyde, ketone, and acidic groups. Their presence may have significant consequences for biomedical coatings produced using DGpp and their possible reactivity toward biological species such as proteins. Surface bound aldehydes and ketones may readily react with amine groups located on many proteins. Residual acid groups on the DGpp surface which we have investigated previously on bulk DGpp surface coatings[56] may also aid in enhancing electrostatic interactions with biomolecules and possibly hinder the performance of these types of coatings in vivo and in vitro. To investigate further any possible reactivity of these residual chemistries the 5 and 30 W gradients (Figure 5C) were incubated with the

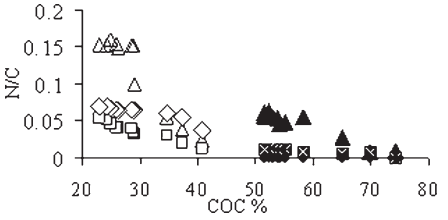

Figure 6. XPS N/C ratios measured after adsorption of BSA (♦), Lys (black box with a white ×), and γ-globulins (▲) as a function of normalized residual ether content in the 5 (solid symbols) and 30 W (hollow symbols) gradients.

amine functional graft copolymer of poly(L-lysine) and poly(ethylene glycol) (PLL-*g*-PEG).[57] It was envisioned that any covalent coupling through covalent reactions of the PLL-*g*-PEG primary amine groups with either aldehydes or ketones and electrostatic interactions with residual acid functionalities may be observed via XPS through the appearance of a nitrogen signal. XPS and NEXAFS surface analysis confirmed that the central region of each gradient was shown to have the lowest aldehyde/ketone and acid/ester components with the 30W generated gradient having the greatest concentration of these species. The assembly on the 5 and 30 W gradients of the polycationic PLL-*g*-PEG (e.g., oppositely charged to the carboxylate presenting DGpp) follows a similar trend to that found for these functionalities indicating there is indeed an interaction of the polymer with these species. It is difficult to categorically deduce whether the polymer is interacting electrostatically, through hydrophobic forces or by formation of covalent bonds with the gradient surfaces. The formation of covalent bonds without specific activation of the carboxylic acid surface functionalities with amine functionalities in the PLL-*g*-PEG is rather unlikely. However, it is possible that there are hydrophobic−hydrophobic interactions occurring between the side chains of the lysine residues with local hydrophobic domains in the DGpp surfaces. The use of PLL-*g*-PEG as a low fouling coating is well documented in the literature and has been reported useful for reducing protein adsorption onto metal oxide surfaces,[57,58] as well as inhibiting bacteria adhesion. Using the surface functionalities introduced across the DGpp gradients during polymerization, we have effectively formed gradients of PLL-*g*-PEG that could be useful in studying the interactions of various proteins, bacteria, and cells and shows the versatility of these PEG-like chemical gradients.

Protein Adsorption. To test the protein adsorption properties of the DGpp gradients, the adsorption of three proteins of varied size and charge (BSA, Lys, and γ-globulin (IgG)) was analyzed via the appearance of nitrogen with XPS (protein detection limit ~10 ng/cm^2). The N/C ratio measured across the 5 and 30 W DGpp gradients was plotted as a function of the actual ether content (COC) of the gradient films (after subtraction of the C−OH contributions via TFAA derivitisation) (Figure 6). By using proteins of varying charge and size at a concentration of 1 mg/mL in PBS, it was hypothesized that we could more thoroughly interrogate the critical parameters related to the production of low fouling PEG-like plasma polymer films. BSA has a net negative charge at physiological pH (p*I* 4.7) and a M_w of ~69 kDa, Lys has a net positive charge at physiological pH (p*I* 11.1) and is a smaller molecule with a molecular weight of ~14.6 kDa, while the IgGs are larger proteins with a molecular weight of ~150 kDa,

(56) Muir, B. W.; Tarasova, A.; Gengenbach, T. R.; Menzies, D. J.; Meagher, L.; Rovere, F.; Fairbrother, A.; McLean, K. M.; Hartley, P. G. *Langmuir* **2008**, *24*(8), 3828–3835.

(57) Blättler, T. M.; Pasche, S.; Textor, M.; Griesser, H. J. *Langmuir* **2006**, *22*(13), 5760–5769.

(58) Pasche, S.; De Paul, S. M.; Janos, V.; Spencer, N. D.; Textor, M. *Langmuir* **2003**, *19*(22), 9216–9225.

an overall neutral charge at physiological pH and p*I* 7.3. The adsorption of each protein systematically increased across the gradients correlating with regions of lower ether content and higher carbonyl, carboxylic acid, and hydrocarbon species, forming adsorbed protein gradients.

The 5W gradient adsorbed no BSA as measured by XPS across its entirety. Lys adsorption was not detected in the central region of the 5 W gradients, however, the N/C ratio increased across the surface gradient at an ether content of less than 70%. The IgGs adsorbed across both the 5 and 30 W gradients with significantly higher amounts detected on the 30 W gradient film. We believe this is in part due to the inherently "sticky" nature of these molecules, their larger size, and the lack of any small contribution from electrostatic repulsion effects under the conditions used in this work. In the center of the 5 W gradient only a small amount of IgG was detected.

A comparison of the adsorption behavior of BSA and Lys on the 30 W gradient showed an opposite situation to that of the 5 W film with more BSA adsorbing than Lys for the former surface. BSA was detected in slightly greater amounts across the 30W gradient with N/C values ranging from 0.012 to 0.056 over a 10 mm distance when compared to the 5 W DGpp gradient. Lys adsorption as measured via the N/C varied from ~0.04 to 0.07. The difference in adsorption behavior of Lys and BSA between the 5 and 30 W gradients may be attributed to such phenomena as increased hydrophobic and electrostatic interactions between the surfaces and proteins. Previous work performed by our group[56] has shown that uniform DGpp films possess an overall negative charge at physiological pH, which in part helps explain one of the mechanisms involved in the low fouling nature of these DGpp coatings along with a high residual ether and low hydrocarbon content. This overall negative surface potential was attributed to species such as surface acid groups. The negative surface potential from these chemical species would help explain the fact that on the 30 W gradient film more Lys adsorbs than BSA. Lys would be expected to interact strongly with negatively charged surface species and this interaction will increase with increasing negative surface potential.[56] Conversely, the fact that BSA adsorbs to a lesser extent across the 30 W gradient film than Lys may in part be due to electrostatic repulsion between the negatively charged protein and gradient surface. Pasche et al[59] has shown that Lys proteins behave in a similar manner to hard, positively charged particles, being attracted by negatively charged surfaces and repelled by positively charged surfaces (on PEGylated Nb_2O_5 surfaces). Analysis of the surface charge across the DGpp gradients should be considered in the future and may confirm stronger negatively charged surfaces in gradients deposited at higher load power, which would help to confirm if it is the electrostatic interactions that are primarily driving the higher Lys adsorption across the 30 W DGpp gradient.

It is clear from the spectroscopic characterization of the films that the 30 W gradient has significantly less ether and more hydrocarbon species along its length. It may be that higher adsorption of BSA across the 30 W gradient coating is driven by hydrophobic−hydrophobic interactions, which may overpower the electrostatic repulsions that occur between BSA proteins and the residual carboxylic acid species across the DGpp gradients. Also, the larger size of BSA compared to Lys, may contribute to a larger number of reactive terminal amine groups that could possibly interact covalently with the residual aldehyde and ketone groups shown to be present across the DGpp gradients from our spectroscopic studies. Further, when Lys does interact with surface defects and chemical entities that are not protein resistant and adsorb on the gradient surfaces, the smaller protein may be more effective at 'blocking' these sites and resisting further immobilization and interaction with additional Lys from solution than BSA.

(59) Pasche, S.; Voros, J.; Griesser, H. J.; Spencer, N. D.; Textor, M. *J. Phys. Chem. B* **2005**, *109*(37), 17545–17552.

Conclusions

A series of PEG-like chemical gradients were prepared using continuous wave radio frequency glow discharge plasma polymerization of diethylene glycol dimethyl ether (DG) at load powers of 5 and 30 W. A knife edge upper electrode was employed to produce the defined chemical gradients studied. Complementary surface analysis techniques were used to characterize the gradients, including grazing incidence-FTIR microspectroscopy, X-ray photoelectron spectroscopy, and near edge X-ray absorption fine structure spectroscopy. We have found that the ether functionality systematically varies across the gradients with the highest "PEG-like" characteristics in the central region of the films deposited directly underneath the razor electrode. It was found that the hydrocarbon, ketone, aldehyde, acid, and ester content varied across the gradients, being lowest in the central region increasing radially outward. Films deposited at 5 W retained higher ether contents and had lower levels of hydrocarbon and carbonyl functionalities than the 30 W gradient films. Adsorbed protein gradients were formed and correlated well with the residual ether content from XPS analysis, with the central region of the gradients being the most protein resistant. Interestingly the observed adsorption trends of the negatively charged BSA and positively charged Lys was reversed across the 5 and 30 W DGpp films. This simple, time-efficient and reproducible method of gradient generation not only produces surfaces that are ideal for the study and characterization of low-fouling films and potentially their subsequent interaction with biomolecules and cells, but could potentially be useful in the generation of gradients presenting other surface functionalities by careful selection of the monomer species used.

Acknowledgment. This research was undertaken on the soft X-ray (NEXAFS, BL6) and infra-red microscope (giFTIR microspectroscopy, BL8) beamlines at the Australian Synchrotron, Victoria, Australia. We thank Kevin Prince for his helpful discussions towards interpretation of the NEXAFS data. We acknowledge the use of the 'Whooshka' software program to perform the curve-fitting of the NEXAFS data. D.J.M. thanks the CSIRO OCE Scheme for funding her Ph.D. scholarship stipend. M.T. acknowledges support from CSIRO's OCE Distinguished Visiting Scientist Program.

Supporting Information Available: Presented is a schematic of the plasma polymer reactor, 2D FTIR surface chemistry plots, and XPS C1s components plotted as a function of distance across the gradients. O K-edge NEXAFS spectra, example C and O curve fits and resulting C and O K-edge curve fit plots. This material is available free of charge via the Internet at http://pubs.acs.org.